Journal of Energy Chemistry 27 (2018) 389–394

Contents lists available at ScienceDirect

Journal of Energy Chemistry

journal homepage: www.elsevier.com/locate/jechem

http://www.journals.elsevier.com/journal-of-energy-chemistry/

Surface-clean low-doped PdB/C as superior electrocatalysts toward ethanol oxidation in alkaline media

Yuan-Fang Wang[1], Chan Zhu[1], Yao-Yue Yang*, Zhi-Gang Zhao

College of Chemistry and Environmental Protection Engineering, Southwest Minzu University, Chengdu 610041, Sichuan, China

ARTICLE INFO

Article history:
Received 16 December 2017
Revised 5 January 2018
Accepted 6 January 2018
Available online 16 January 2018

Keywords:
EOR
Surface-clean
low-doped PdB/C
Alkaline media
Geometric and electronic effects

ABSTRACT

Developing highly active, low-cost and organic surfactants-free Pd-based catalysts for ethanol oxidation reaction (EOR) is now critically important for direct ethanol fuel cells. Herein, surface-clean low-doped PdB/C catalysts (typically ca. 1.5 at% of B) are successfully prepared in an aqueous condition without adding any organic surfactants. TEM characterization shows that as-prepared low-doped PdB nanoparticles are evenly distributed on carbon support. Cyclic voltommagrams of as-prepared low-doped PdB/C in 0.5 M NaOH + 1 M C_2H_5OH indicate that its onset oxidation potential of ethanol is ca. 80–120 mV more negative than that on commercial Pd/C. Meanwhile, the EOR mass activity of our home-made catalysts is up to 4018 $mA \cdot mg^{-1}$ Pd. Moreover, the durability on low-doped PdB/C catalysts is at most 2 times higher than that on commercial Pd/C. Geometric and electronic effects are adopted to understand the above mentioned enhancement of activity and durability. This work may provide a facile, low-cost and green strategy on preparing electrocatalysts toward EOR in alkaline media.

1. Introduction

Recently, ethanol oxidation reaction (EOR) has attracted much attention because direct ethanol fuel cells (DEFCs) are considered as a promising power source for automobile and portable applications [1,2]. Specially, Pd has a comparable activity with Pt for ethanol oxidation reaction (EOR) in alkaline media [2,3] which may make Pd as an alternative to Pt [4,5]. To approach this goal, considerable efforts have been devoted to prepare Pd-based catalysts, including but not limited to Pd nanocrystals [6,7], Pd-metal oxide composites and Pd-based alloy [8–16]. Unfortunately, in these literatures, the complexity of synthetic strategy and post-treatment may limit their wide applications. Moreover, organic surfactants such as polyvinyl pyrrolidone (PVP), cetyltrimethyl ammonium bromide (CTAB), and oleylamine were commonly used as surface capping agents to control particle size and specific surface structure [2,17,18]. Nevertheless, these surface covering surfactants may lead to activity loss for structure-sensitivity reactions [19–22], although several post-treatments (such as UV-Ozone [22], basic bath rinse [23] and CO replacement [6]) have been proposed to solve this issue; a great challenge remains since these cleaning treatment could disrupt underlying surface structures, resulting in distorted electrochemical responses [22,24,25]. Along this line, highly active, low-cost and organic surfactants-free Pd-based catalysts for EOR should be developed.

As for surfactant-free Pd nanoparticles, Burton et al. [26] produced a suspension of Pd nanoparticles using a slow reduction of $Pd(OAc)_2$ in MeOH, but the anhydrous conditions was quite critical and the aggregation of Pd nanoparticles cannot be effectively avoided. Hyotanishi et al. [27] first reported ca. 1.5-nm Pd nanoclusters synthesized by a N,N-dimethylformamide (DMF) reduction method, and the as-prepared Pd nanoclusters showed high catalytic activity in cross-coupling reactions. After that, Li et al. [28] realized a shape-controlled synthesis of Pd nanosheets by simply mixing a dinuclear Pd^I carbonyl chloride complex with H_2O in DMF. Recently, Wang et al. [29] also employed the DMF as solvent to prepared Vulcan XC-72-supported ultrafine Pd catalysts to electroxidize ethanol and formic acid. Nevertheless, their precursor $Pd(acac)_2$ is too expensive. More importantly, DMF containing a free electron pair may also be strongly adsorbed on Pd nanoparticles and interact with surface Pd atoms, tuning the electronic structure of Pd so that the reaction pathway may be modulated. Similar catalytic modulation was observed by Bi et al. when they produced H_2 from formic acid on Au-based catalysts by adding triethylamine [30] or dimethylethanolamine [31] into the reaction solution. Thus, DMF-contained materials seem to lead to uncertainty for the surface-sensitive catalysis. To avoid this, Chen et al. [32] prepared "very clean" ultrafine Pd nanoparticles on graphene

* Corresponding author.
E-mail address: yaoyueyoung@swun.edu.cn (Y.-Y. Yang).
[1] These authors contributed equally to this work.

https://doi.org/10.1016/j.jechem.2018.01.001

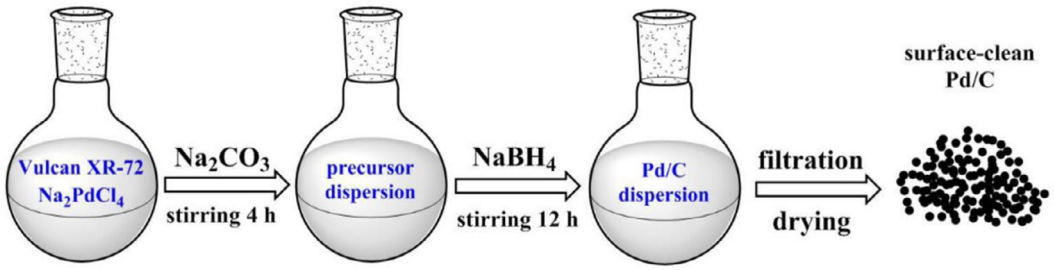

Fig. 1. Schematic illustration of the synthesized process of surface-clean low-doped PdB/C catalysts (no organic surfactants is added).

oxide (GO) surfaces in aqueous condition simply by the redox reaction between $PdCl_4^{2-}$ and GO. The as-made catalyst expressed high electrocatalytic ability in formic acid and ethanol oxidation relative to a commercial Pd/C catalyst. Nevertheless, the durability should be improved owing to the aggregation of ultrafine Pd nanoparticles during the catalytic reactions.

In this work, considering above-mentioned issues, we adopted a facile, green and organic surfactant free routine to prepare surface-clean, high-dispersion B low-doping Pd nanoparticles loaded on Vulcan XC-72. The structural and compositional properties, as well as the catalytic activity and stability of surface-clean PdB/C, were characterized and compared with a commercial Pd/C (Johnson Matthey) catalyst. The enhanced activity and durability for ethanol electro-oxidation in alkaline media was also briefly discussed.

2. Experimental

2.1. Catalysts' preparation and characterization

As shown in Fig. 1, surface-clean low-doped PdB/C catalysts were synthesized according to a modified protocol initially adopted by Zhang et al. [33] targeting for H_2 production from formic acid. In detail, 43 mg of Vulcan XC-72 and 2.23 mL of 45 mM Na_2PdCl_4 were added into 40 mL of Milli-Q water (18.2 MΩ·cm), the mixture was kept under vigorous stirring for ca. 4 h. Then, the solution alkalinity was adjusted to designated pH value by 0.1 M Na_2CO_3 solution. Successively, 10 mL 3 mg/mL $NaBH_4$ + 0.05 M Na_2CO_3 mixture was added dropwise to the suspension with a vigorous stirring by a peristaltic pump at 0.5 mL/min. After 12-hour stirring, the suspension was filtered and washed with copious amounts of Milli-Q water and then dried in vacuum at 323 K overnight. For comparison, the reaction pH was also adjusted to 7.5 and 8.5. The obtained catalysts are denoted as low-doped PdB/C-pH *x* hereafter, where *x* is the pH value of reaction solution.

As-prepared low-doped PdB/C catalysts were detected by a SPECTRO ARCOS inductively coupled plasma-atomic emission spectroscopy (ICP-AES) to analyze the metal loading. The morphology and size distributions of PdB nanoparticles were characterized by a Tecnai G2 F20 transmission electron microscopy (TEM). Electronic and lattice structure was analyzed by a Thermo Fisher K-Alpha X-ray photoelectron spectroscopy (XPS) and a D8 QUEST X-ray diffractometer with Cu K_α radiation (0.15418 nm), respectively.

2.2. Electrochemical measurements

The electrochemical measurement was taken on a CHI 660E electrochemistry workstation with a three-electrode system. A Pt sheet and a saturated calomel electrode (SCE) (or $Hg/HgSO_4$) were employed as the counter and reference electrodes, respectively. The working electrode (WE) was prepared by pipetted a certain amount of catalyst ink that contains 2.0 mg Pd/C, 1.0 mL C_2H_5OH and 120 μL Nafion (5 wt%, Aldrich) onto a freshly polished glassy carbon (GC) electrode. Note that, a 28 μg cm^{-2} of Pd loading on the WE was kept. As for the CO stripping voltammograms, firstly CO (> 99.99% purity) was bubbled and adsorbed onto WE that is immersed in 0.5 M NaOH for 20 min, and then dissolved CO was removed by high purity N_2 flow for at least 1 h. The WE potential was controlled at −0.9 V (SCE) throughout the whole pretreatment process. At last, CO stripping voltammograms were collected at a scan rate of 10 mV s^{-1}. All electrolytes were performed deaeration by bubbling high-purity N_2 before use, and all electrochemical measurements are proceeded at room temperature.

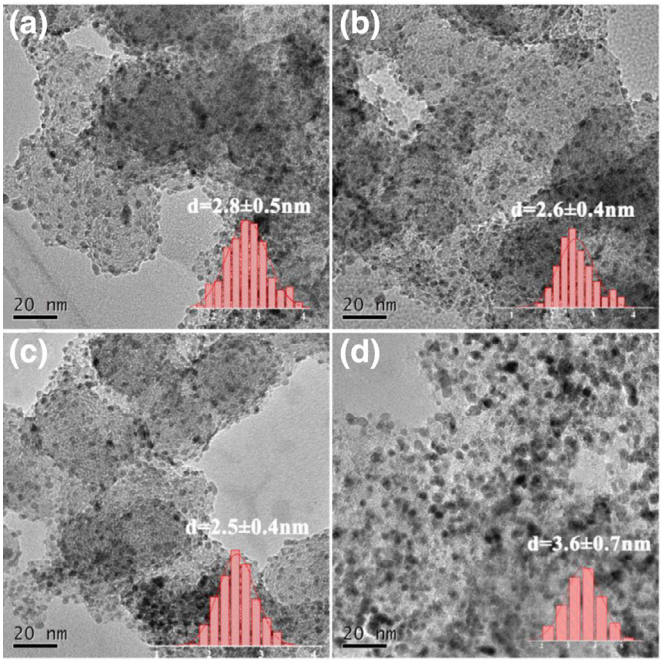

Fig. 2. TEM images and corresponding histograms of Pd particle-size distributions of the as-prepared low-doped PdB/C-pH 9.5 catalyst (a), PdB/C-pH 8.5 catalyst (b), PdB/C-pH 7.5 catalyst (c) and commercial Pd/C (JM) (d).

3. Results and discussion

Particle sizes and distributions of supported nanoparticles are critical parameters influencing the catalytic activity of the materials [34,35]. As a result, the morphologies and particle-size distributions for commercial Pd/C (JM) and as-prepared low-doped PdB/C catalysts were characterized by TEM. As shown in Fig. 2, Pd nanoparticles are uniformly distributed on the carbon support, and nearly no agglomeration is observed. The histograms of particle size and distribution are obtained based on the measurements of 400 nanoparticles in a randomly selected area of the TEM images. Specifically, the average size of as-prepared catalysts is ca. 2.5 ± 0.4 nm (PdB/C-pH 7.5), 2.6 ± 0.4 nm (PdB/C-pH 8.5) and 2.8 ± 0.5 nm (PdB/C-pH 9.5), respectively. This indicates that the

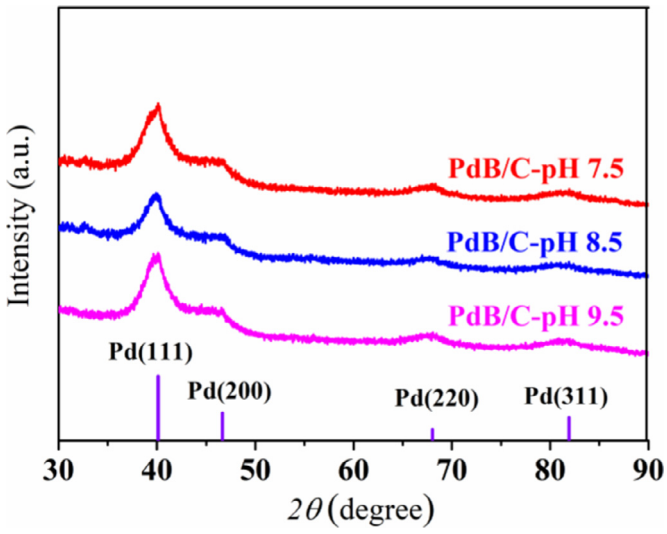

Fig. 3. X-ray diffraction patterns of as-prepared low-doped PdB/C catalysts. The vertical lines are corresponding to the standard angle of face-centered cubic (fcc) Pd (PDF#46-1043).

particle size can be finely regulated by changing the reaction solution pH value.

On the other hand, the particles size can also be estimated by the Scherrer equation [36] $d = 0.9\lambda/B_{2\theta}\cos\theta$, where λ of the Cu K_α radiation is 0.15418 nm, $B_{2\theta}$ employs the half-height width of Pd (111) diffraction peak in radians, θ is the angle of (111) peak. Fig. 3 shows the XRD patterns for series of as-prepared low-doped PdB/C catalysts, where the four peaks correspond to the planes (111), (200), (220) and (311), featuring the face-centered-cubic (fcc) crystalline structure. Thus the average particle size of low-doped PdB/C catalysts is ca. 2.41 nm (PdB/C-pH 7.5), 2.64 nm (PdB/C-pH 8.5) and 2.83 nm (PdB/C-pH 9.5), respectively. These results are in reasonably agreement with those estimated by TEM characterization, although a quantitative comparison was not made.

In addition, a pretty slightly negative shift of Pd(111) peak of as-prepared low-doped PdB/C catalysts is observed, compared with that adapted from PDF#46-1043 for bulk Pd. This may be attributed to an expansion of the Pd lattice through the incorporation of B atoms into the interstice of Pd-Pd lattice spaces, which was also demonstrated elsewhere in literatures [33,37]. Correspondingly, ICP-AES detection of the as-prepared catalysts obtained a ca. 19.1 wt%, ca. 19.7 wt% and ca. 18.9 wt% of Pd loading as well as ca. 1.47 at%, ca. 1.61 at% and ca. 1.53 at% of B doping for as prepared low-doped PdB/C-pH 9.5, PdB/C-pH 8.5 and PdB/C-pH 7.5 catalysts, respectively. The doping of B into Pd-Pd lattice may tune the electronic structure of Pd metal, which will be detailed described in the following.

The ex situ XPS spectra of Pd 3*d* for our home-made low-doped PdB/C and commercial Pd/C were collected to further analyze the surface compositions and valence. As shown in Fig. 4, the Pd 3*d* core levels split into $3d_{5/2}$ (ca. 335 eV) and $3d_{3/2}$ (ca. 340 eV) states because of spin orbital splitting, and both the Pd $3d_{5/2}$ and the Pd $3d_{3/2}$ peaks can be deconvolved into Pd^0 and Pd^{2+} peak. It is worthwhile noticing that the catalysts were exposed under ambient condition before XPS measurements. Hence the presence of Pd^{2+} species may be attributed to the oxidation of Pd active sites [33,38]. From this perspective, the Pd^{2+} to Pd^0 ratio may indicate the numbers of surface active sites that plays a major role in EOR. Therefore, it is reasonable to believe that a catalyst with higher Pd^{2+}/Pd^0 ratio may perform a better catalytic activity, which has been demonstrated on Pd-based catalysts toward H_2 generation from formic acid [33]. Specifically, the Pd^{2+}/Pd^0 ratio of our home-made low-doped PdB/C-pH 9.5, PdB/C-pH 8.5, and PdB/C-pH 7.5 catalysts is ca. 1.7, 1.3 and 1.1 times than that of commercial Pd/C catalyst, indicating highest catalytic activity on low-doped PdB/C-pH 9.5 (vide infra).

Fig. 5(a) shows the cyclic voltammograms (CVs) obtained in 0.5 M NaOH + 1 M C_2H_5OH. It is visible that the onset potential of ethanol oxidation on as-prepared low-doped PdB/C-pH 9.5 moves negatively ca. 120 mV relative to that on commercial Pd/C (JM), being ca. 80 mV lower than that on the commercial catalyst on low-doped PdB/C-pH 7.5 and low-doped PdB/C-pH 8.5.

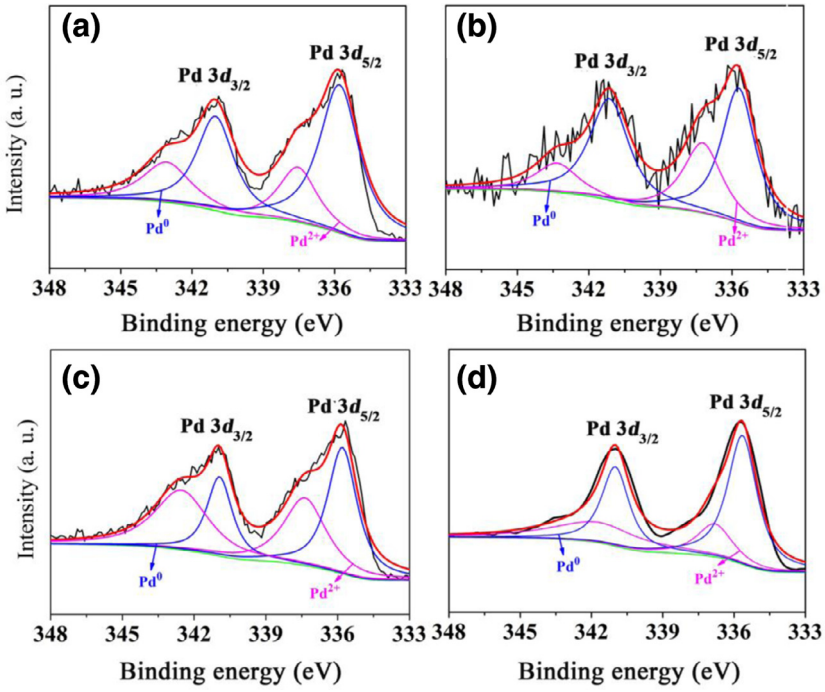

Fig. 4. Core level XPS spectra of Pd 3*d* region for low-doped (a) PdB/C-pH 9.5, (b) PdB/C-pH 7.5, (c) PdB/C-pH 8.5 catalysts and (d) commercial Pd/C-JM catalysts.

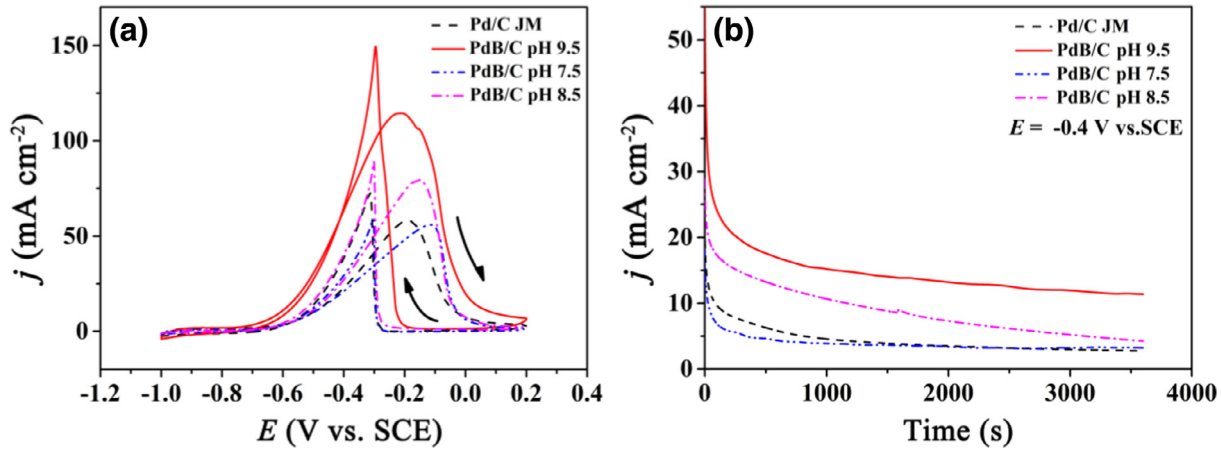

Fig. 5. (a) Cyclic voltammograms (CVs) collected in 0.5 M NaOH + 1 M C_2H_5OH for the as-prepared PdB/C and commercial Pd/C-JM at 50 mV/s; (b) Chronoamperometric curves obtained in 0.5 M NaOH + 1 M C_2H_5OH with the working electrode potential controlled at −0.4 V vs. SCE (the rotated speed of GC is 1000 rpm).

Moreover, 112.5 mA cm^{-2}, 79.8 mA cm^{-2}, 57.2 mA cm^{-2}, 56.8 mA cm^{-2} EOR specific activities could be read on low-doped PdB/C-pH 9.5, PdB/C-pH 8.5, PdB/C-pH 7.5 and PdB/C-JM, respectively, which means the corresponding apparent mass activity is up to ca. 4018 mA·mg^{-1} Pd (low-doped PdB/C-pH 9.5). As shown in Table S1, this value is even much higher than that recently reported 2533 mA·mg^{-1} Pd by Wang et al. over their $Pd_8Ni_1P_1$/C catalysts [39]. Thus, our home-made catalysts may be one of the most active carbon-supported Pd-based catalysts toward EOR so far.

In Fig. 5(b), the durability of our Pd/C-pH 9.5 and commercial Pd/C-JM for EOR was compared. After a 3600-s chronoamperometric test in 0.5 M NaOH + 1 M C_2H_5OH with the potential controlled at −0.4 V vs. SCE, the current density of our home-made Pd/C-pH 9.5 decayed from ca. 55 to ca. 13.5 mA cm^{-2}. In other words, about 25% of the initial current density could be detected. In contrast, the current density of commercial Pd/C at 3600 s is 2.65 mA cm^{-2}, which means only ca. 12.0% of the current density remained after a long-term durability test. Meanwhile, the peak current densities for these two catalysts are around 1.3 times and 1.5 times higher than those of commercial catalysts. The high active electrocatalytic performance indicates that our surface-clean Pd/C may be a promising anode catalyst for practical applications in DEFCs.

CO anodic stripping voltmmagram is generally used to calculate the elelctrochemically active surface active area (ECSA) for nanocatalysts by the following formular:

$$\mathrm{ECSA} = \frac{S}{vm \times 420\ \mu\mathrm{C\ cm^{-2}}}$$

where S is the integral area of CO stripping peak, v is the voltammetric scanning rate and m is the mass of Pd metal coated on the GC electrode surface. And a charge of 420 μC cm^{-2} is assumed for electro-oxidation of the CO monolayer on ideally smooth Pt and Pd surfaces [36,37].

Herein, as shown in Fig. 6, monolayer CO stripping measurements on the as-prepared catalysts were performed. Note that, the asterisk small peak in the second cycle should be attributed to the formation of PdO species rather than the oxidation of residual dissovled CO after our careful confirmation. The estimated ECSA of as-prepared catalysts is 2.67 cm^2 μg^{-1}Pd (Pd/C-pH 9.5), 2.14 cm^2 μg^{-1}Pd (Pd/C-pH 8.5), 1.78 cm^2 μg^{-1}Pd (Pd/C-pH 7.5) and 1.71 cm^2 μg^{-1}Pd (Pd/C-JM), respetively. It is well-known that the larger ECSA was more active for EOR, which was effectively demonstrated by voltammetic study in ethanol containing electrolyte (see Fig. 5).

Finally, it could be considered to empoly the geometric and electronic effects to explain the increasing activity and durability

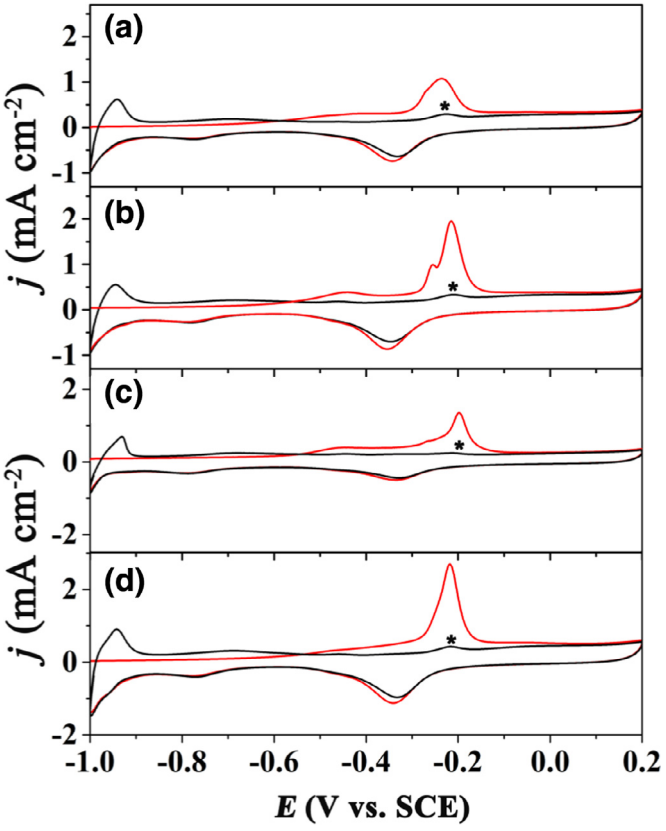

Fig. 6. Monolayer CO stripping voltammograms taken in 0.5 M NaOH on (a) low-doped PdB/C-pH 7.5, (b) low-doped PdB/C-pH 8.5, (c) Pd/C-JM and (d) low-doped PdB/C-pH 9.5 at 10 mV/s. The red and black lines are corresponding to the first and second scan cycles, respectively.

for EOR on our home-made PdB/C catalysts in alkaline media based on above characterizatons and discussions.

Regarding the gemoetric effects, above-described ex-situ XPS measurements showed that the Pd^{2+}/Pd^0 ratio of home-made low-doped PdB/C-pH 9.5, PdB/C-pH 8.5, and PdB/C-pH 7.5 catalysts is ca. 1.7, 1.3 and 1.1 times than that of commercial Pd/C catalyst respectively, indicating more surface active sites on home-made low-doped PdB/C catalysts surface. More directly, the estimated ECSA through CO stripping voltammograms of PdB/C was ca. 1.1 to 1.5-

Table 1. The comparison of various parameters for the four catalysts in this work.

Catalysts	Mean particle size (nm)	N_s/N_t	Activity (mA cm^{-2})	ECSA (cm^2 μg^{-1}Pd)
PdB/C-pH 9.5	ca.2.8	0.44	112.5	2.67
PdB/C-pH 8.5	ca.2.6	0.47	79.8	2.14
PdB/C-pH 7.5	ca. 2.5	0.48	57.2	1.78
Pd/C-JM	ca. 3.6	0.35	56.8	1.71

time larger than commercial Pd/C (as shown in Table 1). Thus a better EOR catalytic performance on our low-doped PdB/C catalysts could be logically and readily understood.

On the other hand, we try to adopt the ratio of surface atoms to total atoms of the nanoparticles (namely N_s/N_t value) to understand the size effect, which may be helpful to understand the catalysis difference between our as-prepared catalysts and the commercial catalyst. N_s/N_t value could be estimately calculated through a previously reported method using an thermodynamically stable cuboctahedron model [33,40]. In detail, the nanoparticles are formed by onion-like concentric atomic layers around a single central atom, and the central atom was counted as the first shell. The total number of atoms (N_t) was expressed as $N_s = 10\ m^2 - 20\ m + 12$, where m is the number of atomic layers and equals to $2.2d$ (here d is the average particle diameter). And the number of surface atoms (N_s), i.e. the mth atomic layer, was expressed as $N_t = 0.33(2m-1)(5m^2-5m+3)$. According to Table 1, the N_s/N_t ratio of as-prepared low-doped PdB/C is bigger than that of Pd/C-JM, suggesting that our home-made catalysts may provide more surface active sites for EOR. However, this mode might be unable to explain why the three as-prepared PdB/C catalysts have obvious difference, which has been disscused by ECSA difference above. Hence, the investigation on the surface structure difference of as-prepared three low-doped PdB/C catalysts should be carried out sequentially.

As for the electronic effects, given that the size difference between Pd nanoparticles is insufficient to account for the activity gap between as-prepared low-doped PdB/C and the Pd/C-JM catalysts, the B-doping is assumed to be more relevant. Note that, B was extensively used for modifying the physicochemical properties of the functional materials [41,42]. Boron atoms are much smaller than Pd atoms, which may incorporate into Pd-Pd interlattice spaces rather than substitute Pd atoms. According to the so-called d-band centre theory [43–45], the interstitial incorporation of B atoms into the Pd lattice should cause the downshift of Pd d-band center, due to the covalent bonding between the Pd 3*d* states and the B 2*p* states. Meanwhile, d-band center shifting could modurate the surface absorption energy of reaction intermediates [46], as a result, the reaction pathway and mechanism of surface-sensitive reactions might change. This has been demonstrated on Pd-based catalysts toward formic acid electrooxidation [36,37,47]. In fact, a suitable down-shift of d-band center is widely accepted to enhance the catalytic performance of formic acid oxidation on Pd [36–38,47], which was understood by easy removal of the poision intermediates, i.e., surface adsorbed CO species (COad). However, in EOR COad is recognized as an important reactive intermediate of C1 reaction pathway [2,48,49]. Meanwhile, Kopper's group also pointed out that COad could serve as a promoter of ethanol oxidation in alkaline media [50]. Thus, proper shifting *D D*-band center postively may increase the EOR activity of low-doped PdB/C catalysts. Note that, it is reported that the d-band centre shift towards fermi level energy when the particle size decrease [51]. Hence the adsorption energy of surface species on low-doped PdB/C is stronger than that on commercial Pd/C, which could also largely benefit ethanol oxidation according to above discussion.

4. Conclusions

In summary, surface-clean low-doped PdB/C catalysts were successfully prepared through a facial and green routine. On our hommade low-doped PdB/C catalysts, the mass activity of EOR in alkaline media was as high as ca. 4018 $mA \cdot mg^{-1}$Pd, and a pronounced durability for EOR was also obtained. It is believed that geometric and electronic effects should be responsible for the enhanced the catalytic performance. This work may provide some new thoughts about the preparation of high-efficiency and low-cost EOR catalysts.

Acknowledgments

This work was supported by NSFC (No.21603177), the Natural Science Foundation of Sichuan Province (No.2016JY0212), the Fundamental Research Funds for the Central Universities (No.2017NGJPY05) and the Innovation Funds for SMU students (No. 201710656023). In addition, we sincerely thank Prof. Wen-Bin Cai from Fudan University for the advices on the synthesis of surface-clean Pd nanoparticles.

Supplementary materials

Supplementary material associated with this article can be found, in the online version, at doi:10.1016/j.jechem.2018.01.001.

References

[1] A. Rabis, P. Rodriguez, T.J. Schmidt, ACS Catal. 2 (2012) 864–890.
[2] C. Bianchini, P.K. Shen, Chem. Rev. 109 (2009) 4183–4206.
[3] E. Antolini, E.R. Gonzalez, J. Power Sources 195 (2010) 3431–3450.
[4] X.L. Tian, L.J. Wang, P.L. Deng, Y. Chen, B.Y. Xia, J. Energy Chem. 26 (2017) 1067–1076.
[5] X.L. Tian, Y.Y. Xu, W.Y. Zhang, T. Wu, B.Y. Xia, X. Wang, ACS Energy Lett. 2 (2017) 2035–2043.
[6] H.X. Zhang, H. Wang, Y.S. Re, W.B. Cai, Chem. Commun. 48 (2012) 8362–8364.
[7] L. Ma, D. Chu, R.R. Chen, Int. J. Hydrog. Energy 37 (2012) 11185–11194.
[8] Y. Wang, F.-F. Shi, Y.-Y. Yang, W.-B. Cai, J. Power Sources 243 (2013) 369–373.
[9] W.X. Du, K.E. Mackenzie, D.F. Milano, N.A. Deskins, D. Su, X.W. Teng, ACS Catal. 2 (2012) 287–297.
[10] S.Y. Shen, T.S. Zhao, J.B. Xu, Y.S. Li, J. Power Sources 195 (2010) 1001–1006.
[11] J.B. Xu, T.S. Zhao, S.Y. Shen, Y.S. Li, Int. J. Hydrog. Energy 35 (2010) 6490–6500.
[12] E. Antolini, Energ. Environ. Sci. 2 (2009) 915–931.
[13] P.K. Shen, C.W. Xu, Electrochem. Commun. 8 (2006) 184–188.
[14] Y.R. Ma, T.F. Li, H. Chen, X.J. Chen, S.H. Deng, L. Xu, D.M. Sun, Y.W. Tang, J. Energy Chem. 26 (2017) 1238–1244.
[15] T. Yuan, A.J. Wang, K.M. Fang, Z.G. Wang, J.J. Feng, J. Energy Chem. 26 (2017) 1231–1237.
[16] P. Zhang, Y. Wei, J. Cai, Y.X. Chen, Z.Q. Tian, Chin. J. Catal. 37 (2016) 1156–1165.
[17] D. Astruc, F. Lu, J.R. Aranzaes, Angew. Chem. Int. Edit. 44 (2010) 7852–7872.
[18] S.W. Kim, J. Park, Y. Jang, Y. Chung, S. Hwang, T. Hyeon, Y.W. Kim, Nano Lett. 3 (2014) 1289–1291.
[19] D. Li, C. Wang, D. Tripkovic, S. Sun, N.M. Markovic, V.R. Stamenkovic, ACS Catal. 2 (2012) 1358–1362.
[20] J.Y. Park, C. Aliaga, J.R. Renzas, H. Lee, G.A. Somorjai, Catal. Lett. 129 (2009) 1–6.
[21] N. Tian, Z.Y. Zhou, N.F. Yu, L.Y. Wang, S.G. Sun, J. Am. Chem. Soc. 132 (2010) 7580–7581.
[22] F.J. Vidal-Iglesias, J. Solla-Gullón, E. Herrero, V. Montiel, A. Aldaz, J.M. Feliu, Electrochem. Commun. 13 (2011) 502–505.
[23] F.J. Vidaliglesias, R.M. Aránais, J. Sollagullón, E. Herrero, J.M. Feliu, ACS Catal. 2 (2012) 901–910.
[24] J. Sollagullón, F.J. Vidaliglesias, J.M. Feliu, Ann. Rep. Sect. C (Phys. Chem.) 107 (2011) 263–297.
[25] M. Crespo-Quesada, J.-M. Andanson, A. Yarulin, B. Lim, Y. Xia, L. Kiwi-Minsker, Langmuir 27 (2011) 7909–7916.
[26] P.D. Burton, T.J. Boyle, A.K. Datye, J. Catal. 280 (2011) 145–149.
[27] M. Hyotanishi, Y. Isomura, H. Yamamoto, H. Kawasaki, Y. Obora, Chem. Commun. 47 (2011) 5750–5752.
[28] H. Li, G. Chen, H. Yang, X. Wang, J. Liang, P. Liu, M. Chen, N. Zheng, Ang. Chem. Inter.l Ed. 52 (2013) 8368–8372.
[29] Q. Wang, Y. Liao, H. Zhang, J. Li, W. Zhao, S. Chen, J. Power Sources 292 (2015) 72–77.
[30] Q.Y. Bi, X.L. Du, Y.M. Liu, Y. Cao, H.Y. He, K.N. Fan, J. Am. Chem. Soc. 134 (2012) 8926–8933.
[31] Q.Y. Bi, J.D. Lin, Y.M. Liu, F.Q. Huang, Y. Cao, Int. J. Hydrog. Energy 41 (2016) 21193–21202.

[32] X. Chen, G. Wu, J. Chen, X. Chen, Z. Xie, X. Wang, J. Am. Chem. Soc. 133 (2011) 3693–3695.
[33] S. Zhang, B. Jiang, K. Jiang, W.B. Cai, ACS Appl. Mater. Inter. 9 (2017) 24678–24687.
[34] W.P. Zhou, A. Lewera, R. Larsen, R.I. Masel, P.S. Bagus, A. Wieckowski, J. Phys. Chem. B 110 (2006) 13393–13398.
[35] W.J. Zhou, J.Y. Lee, J. Phys. Chem. C 112 (2008) 3789–3793.
[36] H.X. Zhang, C. Wang, J.Y. Wang, J.J. Zhai, W.B. Cai, J. Phys. Chem. C 114 (2010) 6446–6451.
[37] J.Y. Wang, Y.Y. Kang, H. Yang, W.B. Cai, J. Phys. Chem. C 113 (2009) 8366–8372.
[38] K. Jiang, J. Chang, H. Wang, S. Brimaud, W. Xing, R.J. Behm, W.B. Cai, ACS Appl. Mater. Inter. 8 (2016) 7133–7138.
[39] Y. Wang, F.F. Shi, Y.Y. Yang, W.B. Cai, J. Power Sources 243 (2013) 369–373.
[40] Y. Zhang, Y.C. Hsieh, V. Volkov, D. Su, W. An, R. Si, Y. Zhu, P. Liu, J.X. Wang, R.R. Adzic, ACS Catal. 4 (2016) 738–742.
[41] X.B. Yu, M.H. Wang, H.X. Li, Appl. Catal. A Gen. 202 (2000) 17–22.
[42] J.F. Geng, D.A. Jefferson, B.F.G. Johnson, Chem. Commun. (2007) 969–971.
[43] A. Ruban, B. Hammer, P. Stoltze, H.L. Skriver, J.K. Nørskov, J. Mol. Catal. A: Chem. 115 (1997) 421–429.
[44] B. Hammer, J.K. Nørskov, Adv. Catal. 45 (2000) 71–129.
[45] J. Greeley, J.K. Nørskov, M. Mavrikakis, Annu. Rev. Phys. Chem. 53 (2002) 319–348.
[46] L.A. Kibler, A.M. El-Aziz, R. Hoyer, D.M. Kolb, Angew. Chem. Int. Edit. 44 (2005) 2080–2084.
[47] U.B. Demirci, J. Power Sources 173 (2007) 11–18.
[48] Y.Y. Yang, J. Ren, Q.X. Li, Z.Y. Zhou, S.G. Sun, W.B. Cai, ACS Catal. 4 (2014) 798–803.
[49] Y. Wang, S. Zou, W.B. Cai, Catalysts 5 (2015) 1507–1534.
[50] P. Rodriguez, Y. Kwon, M.T. Koper, Nat. Chem. 4 (2012) 177–182.
[51] W.P. Zhou, A. Lewera, R. Larsen, R.I. Masel, P.S. Bagus, A. Wieckowski, J. Phys. Chem. B 110 (2006) 13393–13398.